NASA/TM—2006-214100

Mechanical Characterization of ZnSe Windows for Use With the Flow Enclosure Accommodating Novel Investigations in Combustion of Solids (FEANICS) Module

Jonathan A. Salem
Glenn Research Center, Cleveland, Ohio

February 2006

The NASA STI Program Office . . . in Profile

Since its founding, NASA has been dedicated to the advancement of aeronautics and space science. The NASA Scientific and Technical Information (STI) Program Office plays a key part in helping NASA maintain this important role.

The NASA STI Program Office is operated by Langley Research Center, the Lead Center for NASA's scientific and technical information. The NASA STI Program Office provides access to the NASA STI Database, the largest collection of aeronautical and space science STI in the world. The Program Office is also NASA's institutional mechanism for disseminating the results of its research and development activities. These results are published by NASA in the NASA STI Report Series, which includes the following report types:

- TECHNICAL PUBLICATION. Reports of completed research or a major significant phase of research that present the results of NASA programs and include extensive data or theoretical analysis. Includes compilations of significant scientific and technical data and information deemed to be of continuing reference value. NASA's counterpart of peer-reviewed formal professional papers but has less stringent limitations on manuscript length and extent of graphic presentations.

- TECHNICAL MEMORANDUM. Scientific and technical findings that are preliminary or of specialized interest, e.g., quick release reports, working papers, and bibliographies that contain minimal annotation. Does not contain extensive analysis.

- CONTRACTOR REPORT. Scientific and technical findings by NASA-sponsored contractors and grantees.

- CONFERENCE PUBLICATION. Collected papers from scientific and technical conferences, symposia, seminars, or other meetings sponsored or cosponsored by NASA.

- SPECIAL PUBLICATION. Scientific, technical, or historical information from NASA programs, projects, and missions, often concerned with subjects having substantial public interest.

- TECHNICAL TRANSLATION. English-language translations of foreign scientific and technical material pertinent to NASA's mission.

Specialized services that complement the STI Program Office's diverse offerings include creating custom thesauri, building customized databases, organizing and publishing research results . . . even providing videos.

For more information about the NASA STI Program Office, see the following:

- Access the NASA STI Program Home Page at ***http://www.sti.nasa.gov***

- E-mail your question via the Internet to help@sti.nasa.gov

- Fax your question to the NASA Access Help Desk at 301–621–0134

- Telephone the NASA Access Help Desk at 301–621–0390

- Write to:
  NASA Access Help Desk
  NASA Center for AeroSpace Information
  7121 Standard Drive
  Hanover, MD 21076

NASA/TM—2006-214100

Mechanical Characterization of ZnSe Windows for Use With the Flow Enclosure Accommodating Novel Investigations in Combustion of Solids (FEANICS) Module

Jonathan A. Salem
Glenn Research Center, Cleveland, Ohio

National Aeronautics and
Space Administration

Glenn Research Center

February 2006

Acknowledgments

The author thanks NASA's Human System Research and Technology Office for funding this work, and Abhishek Singh, Summer High School Apprenticeship Research Program (SHARP), for measuring the branch lengths and the hardness.

Available from

NASA Center for Aerospace Information
7121 Standard Drive
Hanover, MD 21076

National Technical Information Service
5285 Port Royal Road
Springfield, VA 22100

Available electronically at http://gltrs.grc.nasa.gov

Mechanical Characterization of ZnSe Windows for Use With the Flow Enclosure Accommodating Novel Investigations in Combustion of Solids (FEANICS) Module

Jonathan A. Salem
National Aeronautics and Space Administration
Glenn Research Center
Cleveland, Ohio 44135

Abstract

Young's modulus, Poisson's ratio, equibiaxial fracture strength, inherent crack size, grain size, hardness and the branching constant of ZnSe windows to be used with the FEANICS (Flow Enclosure Accommodating Novel Investigations in Combustion of Solids) experiments were measured in order to determine design allowables. The average Young's modulus, Poisson's ratio, equibiaxial fracture strength, flaw size, grain size, Knoop hardness, Vicker's hardness, and branching constant were E = 74.3±0.1 GPa, ν = 0.31, $\overline{\sigma}_f$ = 57.8±6.5 MPa, a = 21±4 μm, $\bar{l}$ = 43±9 μm, HK0.5/15 = 0.97±0.02 GPa, HV0.5/15 = 0.97±0.02 GPa, and A_b = 1.0±0.1 MPa√m. The properties of current ZnSe made by chemical vapor deposition are in good agreement with those measured in the 1970's. The hardness of CVD ZnSe windows is about one-twentieth of the sapphire window being replaced, and about one-sixth of that of window glass. Thus the ZnSe window must be handled with great care. The large grain size relative to the inherent crack size implies the need to use single crystal crack growth properties in the design process. In order to determine the local failure stresses in one of the test specimens, a solution for the stresses between the support ring and the edge of a circular plate load between concentric rings was derived.

Introduction

The International Space Station FEANICS (Flow Enclosure Accommodating Novel Investigations in Combustion of Solids) module is designed to perform various combustion experiments in zero gravity. The module fits into the Combustion Integrated Rack (CIR) of the Fluids and Combustion Facility (FCF) and is observed via eight CIR sapphire windows shown in figure 1. FEANICS intends to replace one of those windows with a 63-mm-diameter CVD (chemical vapor deposition) ZnSe (zinc selenide) window which will allow a laser beam of 10.6 μm wavelength to pass. Both FEANICS and CIR are being developed at the NASA Glenn Research Center, Cleveland, Ohio.

ZnSe is a soft, weak ceramic that exhibits crack growth in the presence of water. Further, its strength depends on grain size. A recent review of the literature on CVD ZnSe indicated that much of the crack growth and fracture strength data was generated during the 1970's (ref. 1) with commercial grades which no longer exist. The reported fracture strength was greater than 50 MPa with a Weibull modulus of 9 for well prepared test specimens. In order to verify the mechanical properties of the CVD ZnSe[1] window material being used for viewing the FEANICS module, fracture strength, grain size and other properties were measured and are archived in this report as part of the NASGRO[2] design process.

[1]CVD Zinc Selenide, (Rohm and Haas, Woburn, Massachusetts)
[2]NASGRO Fracture Mechanics and Fatigue Crack Growth Analysis Software Version 4.2, May, 2005. www.nasgro.swri.org. Also, see NASA SSP 30560.

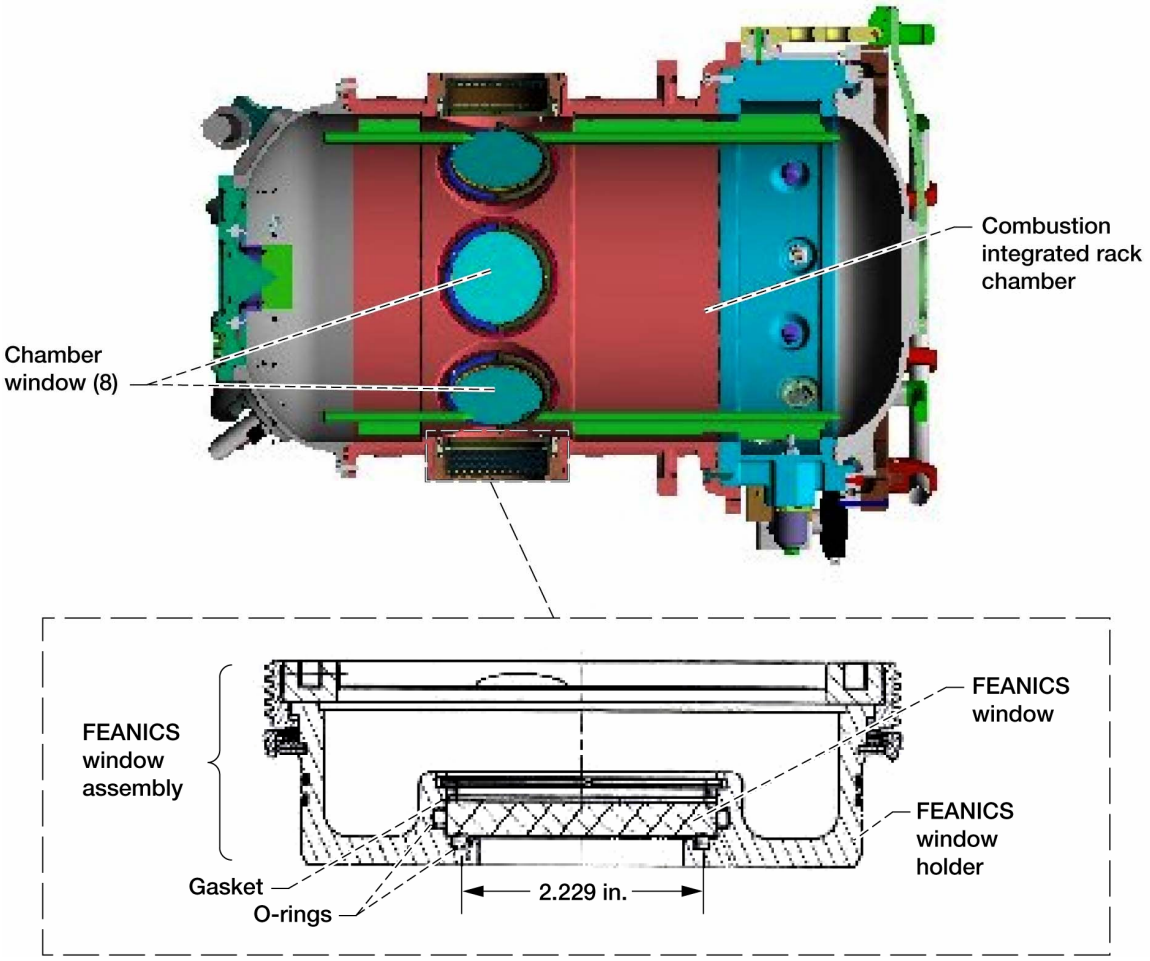

Figure 1.—Combustion Integrated Rack and ZnSe window assembly for use with the FEANICS module.

Test Specimen Preparation and Inspection

Circular plates of the CVD ZnSe to be used with the FEANICS module were prepared according to the drawing and specifications in figure 2, which were developed for the actual windows, with one exception: the thickness of the test specimens was reduced to 4 mm to comply with American Society for Testing and Materials (ASTM) C1499 (ref. 2). Optical inspection of the edges at ~10× indicated an excellent edge-finish with no apparent chips. Some details of the polishing procedure are given in the appendix. Additional tests on witness specimens to be manufactured along with the actual window are planned.

Elastic Properties

Young's modulus and Poisson's ratio were determined at room temperature in accordance with ASTM C1259 (ref. 3) by using an automated linear interpolation routine (ref. 4). The average modulus and Poisson's ratio were $E = 74.3 \pm 0.1$ GPa and $\nu = 0.31 \pm 0.001$, respectively, as shown in table 1. This is slightly higher than some of the reported values (69 to 72.4 GPa (ref. 1)), likely due to the use of a sonic technique as compared to a strain gage. The average bulk density was required for estimation of the elastic properties. The measured value was 5.25±0.003 g/cc.

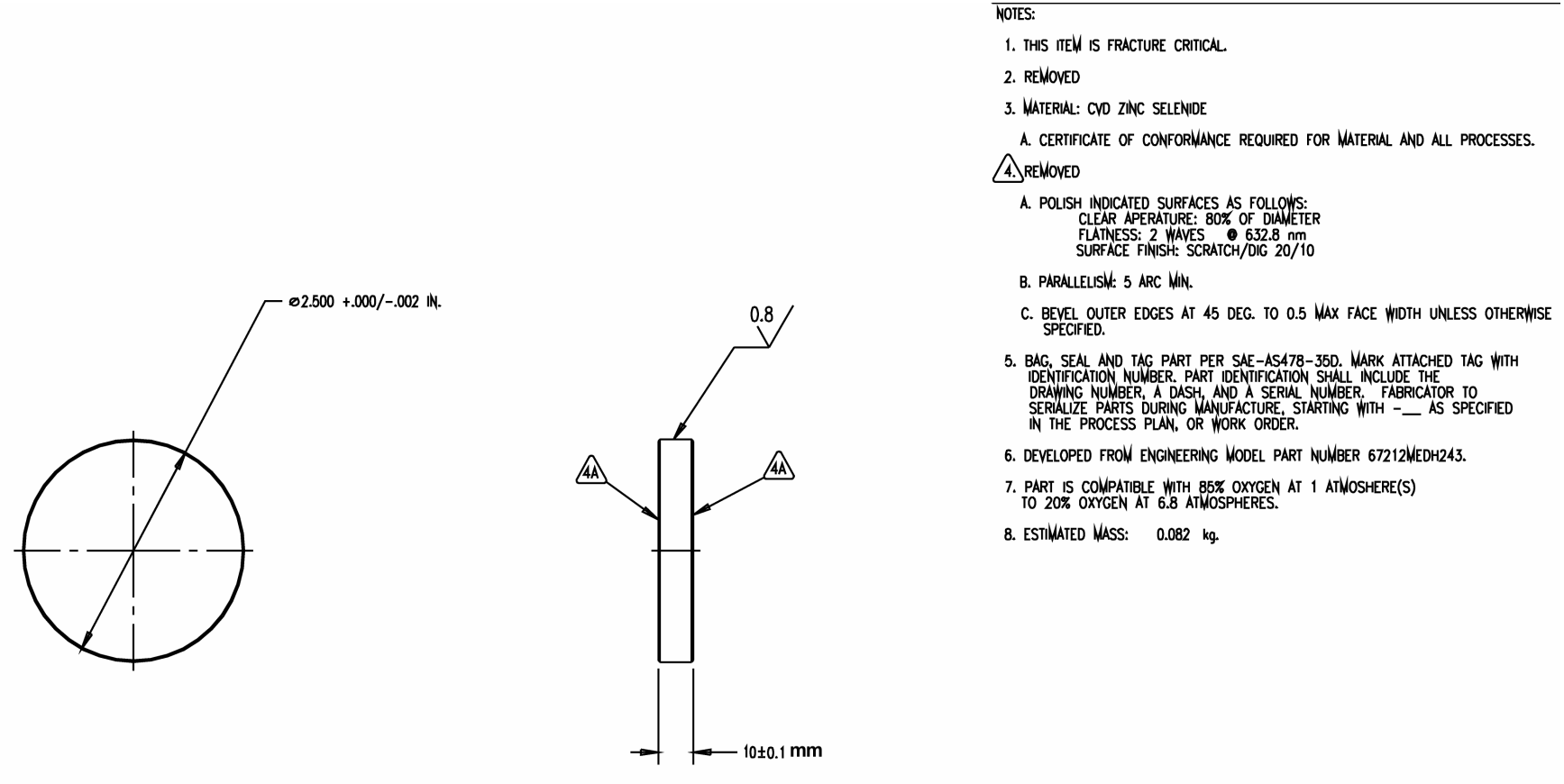

NOTES:

1. THIS ITEM IS FRACTURE CRITICAL.
2. REMOVED
3. MATERIAL: CVD ZINC SELENIDE

   A. CERTIFICATE OF CONFORMANCE REQUIRED FOR MATERIAL AND ALL PROCESSES.

4. REMOVED

   A. POLISH INDICATED SURFACES AS FOLLOWS:
      CLEAR APERATURE: 80% OF DIAMETER
      FLATNESS: 2 WAVES @ 632.8 nm
      SURFACE FINISH: SCRATCH/DIG 20/10

   B. PARALLELISM: 5 ARC MIN.

   C. BEVEL OUTER EDGES AT 45 DEG. TO 0.5 MAX FACE WIDTH UNLESS OTHERWISE SPECIFIED.

5. BAG, SEAL AND TAG PART PER SAE-AS478-35D. MARK ATTACHED TAG WITH IDENTIFICATION NUMBER. PART IDENTIFICATION SHALL INCLUDE THE DRAWING NUMBER, A DASH, AND A SERIAL NUMBER. FABRICATOR TO SERIALIZE PARTS DURING MANUFACTURE, STARTING WITH -__ AS SPECIFIED IN THE PROCESS PLAN, OR WORK ORDER.
6. DEVELOPED FROM ENGINEERING MODEL PART NUMBER 67212MEDH243.
7. PART IS COMPATIBLE WITH 85% OXYGEN AT 1 ATMOSHERE(S) TO 20% OXYGEN AT 6.8 ATMOSPHERES.
8. ESTIMATED MASS: 0.082 kg.

Figure 2.—Specification for biaxial strength test specimens and FEANICS window.

TABLE 1.—YOUNG'S MODULUS AND POISSON'S RATIO OF ROHM AND HAAS CVD ZnSe.

Specimen number	Specimen thickness, h mm	Specimen diameter, D mm	Specimen mass, g	Flexural frequency, f_2 Hz	Torsional frequency, f_1 Hz	Density, ρ g/cc	Poisson's ratio, v	f_2/f_1	h/r	Young's modulus, E GPa
Tag 27335:										
1RH	4.025	63.52	66.8689	6390	3790	5.243	0.31	1.686	0.127	74.4
2RH	4.036	63.50	67.0314	6430	3800	5.244	0.31	1.692	0.127	74.4
3RH	4.027	63.52	66.9133	6410	3790	5.244	0.31	1.691	0.127	74.5
4RH	4.002	63.53	66.5884	6350	3760	5.250	0.31	1.689	0.126	74.2
5RH	4.006	63.52	66.6160	6350	3760	5.248	0.31	1.689	0.126	74.0
6RH	4.057	63.55	67.5582	6433	3810	5.250	0.31	1.688	0.128	74.3
7RH	4.052	63.53	67.4034	6421	3810	5.248	0.31	1.685	0.128	74.3
8RH	4.037	63.55	67.1861	6393	3790	5.248	0.31	1.687	0.127	74.2
9RH	4.033	63.53	67.0277	6407	3790	5.243	0.31	1.691	0.127	74.2
10RH	4.003	63.56	66.6818	6344	3760	5.250	0.31	1.687	0.126	74.3
11RH	4.037	63.39	66.8498	6430	3810	5.248	0.31	1.688	0.127	74.2
12RH	4.042	63.53	67.2197	6425	3800	5.246	0.31	1.691	0.127	74.4
13RH	4.022	63.53	66.8277	6403	3790	5.242	0.31	1.689	0.127	74.6
14RH	4.035	63.52	67.1737	6395	3790	5.253	0.31	1.687	0.127	74.2
15RH	4.005	63.53	66.6289	6356	3770	5.248	0.31	1.686	0.126	74.4
16RH	4.007	63.52	66.6571	6373	3770	5.250	0.31	1.690	0.126	74.4
Tag 27460:										
17RH	3.938	63.53	65.5723	6250	3700	5.253	0.31	1.689	0.124	74.2
18RH	3.936	63.53	65.5447	6250	3700	5.253	0.31	1.689	0.124	74.2
19RH	3.937	63.52	65.4160	6270	3710	5.244	0.31	1.690	0.124	74.5
20RH	3.967	63.53	66.0247	6290	3730	5.250	0.31	1.686	0.125	74.2
21RH	3.926	63.55	65.3782	6230	3690	5.250	0.31	1.688	0.124	74.3
22RH	3.949	63.52	65.6696	6300	3720	5.248	0.31	1.694	0.124	74.6
23RH	3.963	63.56	66.0175	6283	3720	5.251	0.31	1.689	0.125	74.2
24RH	3.973	63.51	66.0248	6330	3740	5.246	0.31	1.693	0.125	74.4
25RH	3.935	63.53	65.4649	6263	3710	5.248	0.31	1.688	0.124	74.6
								Average = 74.3±0.1GPa		

Fracture Strength

Fracture strength of the CVD ZnSe to be used with the FEANICS module was determined by loading circular plates between two concentric rings in accordance with ASTM C1499 (ref. 2). The strength tests were performed in distilled, deionized water at an average stress rate of 10.2 MPa/s. A summary report on the testing details is given in the appendix.

The measured mean equibiaxial fracture strength was $\overline{\sigma}_f$ = 57.8±6.5 MPa, as shown in table 2. The Weibull modulus, *m*, and characteristic strength,σ_θ, as estimated with the maximum likelihood estimator were 9.6 and 60.6 MPa, respectively. The values as estimated by rank regression were 10.9 and 60.3 MPa, respectively. A Weibull plot of the data is shown in figure 3, and examples of failed test specimens are shown in figure 4.

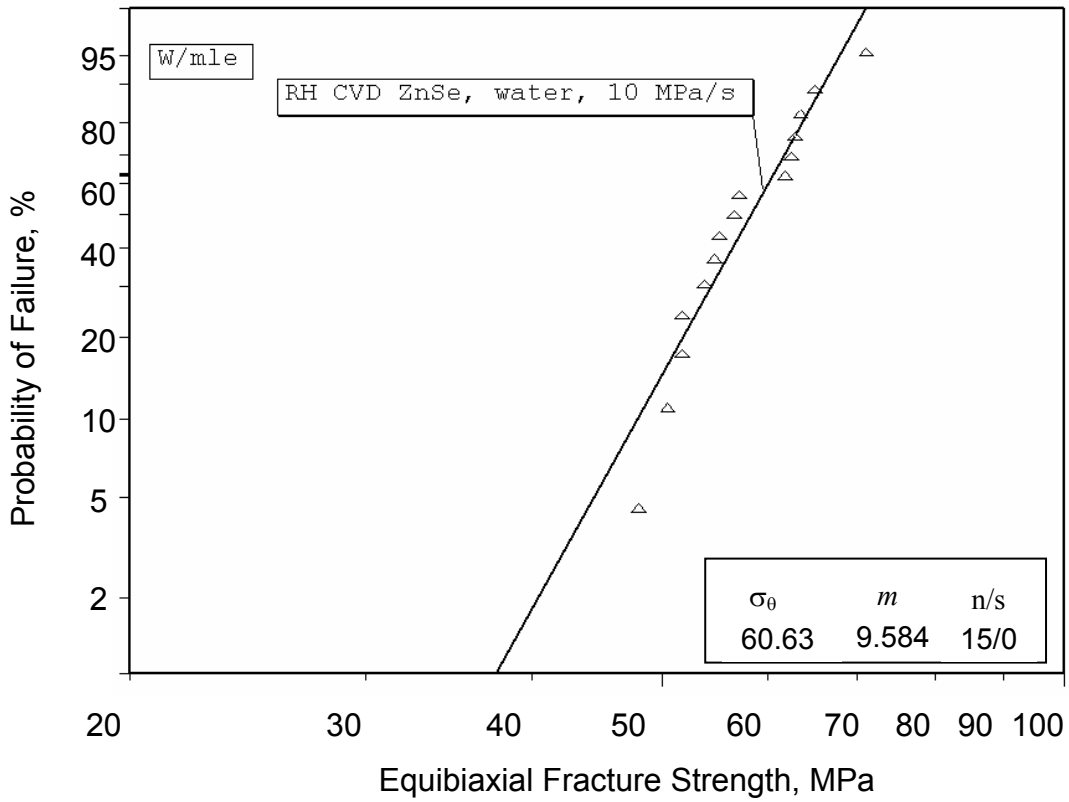

Figure 3.—Weibull plot of the equibiaxial fracture strength of CVD ZnSe.

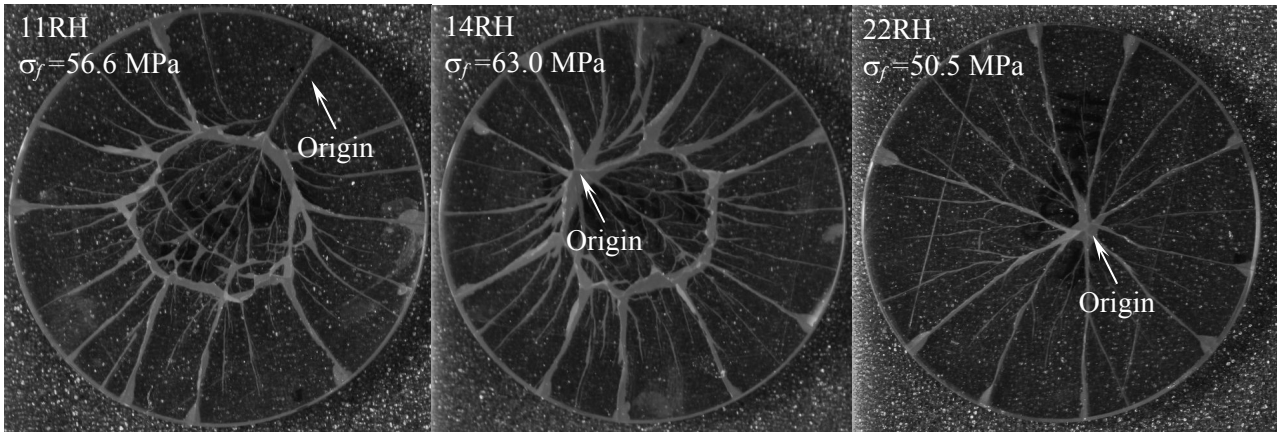

Figure 4.—Example failure origins in 63.5 mm diameter CVD ZnSe test specimens.

These results compare well with the data generated by point loading of circular plates supported with three balls (BO3B) (refs. 1 and 5) and large four-point bend (4PB) tests, as shown in figure 5. For BO3B tests run in water at stress rates of 75 and 0.075 MPa/s, the mean strengths were 56.1±10.1 MPa and 49.1±8.6 MPa, respectively (ref. 1). For 139 large 4PB tests in 45 percent RH (relative humidity) air, the mean strength was 52.3±6.9 MPa, the Weibull modulus was 9.23, and the characteristic strength was 54.3 MPa (refs. 1 and 6). Small, poorly machined 4PB beams exhibited significantly lower strength as shown in figure 5 (ref. 1).

The test specimen effective surface area, A_e, and characteristic fracture strength for the large 4PB and ROR tests were not correlated according to the usual formula

$$\frac{\sigma_{\theta 1}}{\sigma_{\theta 2}} = \left(\frac{A_{e2}}{A_{e1}} \right)^{1/m} \tag{1}$$

despite the Weibull moduli being very similar. Based on equation (1) and the large 4PB data, the expected characteristic strength of the ROR tests was 48.0 MPa as compared to 60.3 MPa. Evidently, differences in manufacturing resulted in different strength levels despite the similar Weibull moduli.

Crack Size

The measured fracture strengths can be used to estimate the flaws sizes of the strength test specimens by assuming that the maximum principal stress and single crystal fracture toughness result in mode I failures. Crack lengths corresponding to the maximum stress intensity for both a long shallow crack with $a/c = 0.1$ and a half-penny crack ($a = c$) were estimated and are tabulated in table 2. The estimated crack lengths, with the exception of one value for a specimen that failed from an unusually large flaw, are invariably less than the average grain size, implying that single crystal properties will dominate crack growth. The test specimen that failed from an unusually large flaw (no. 11 RH) was not included in estimating an average inherent flaw size of $a = 21 \pm 4$ μm. Because the fracture strength measurements were made in water, the initial crack sizes were somewhat smaller.

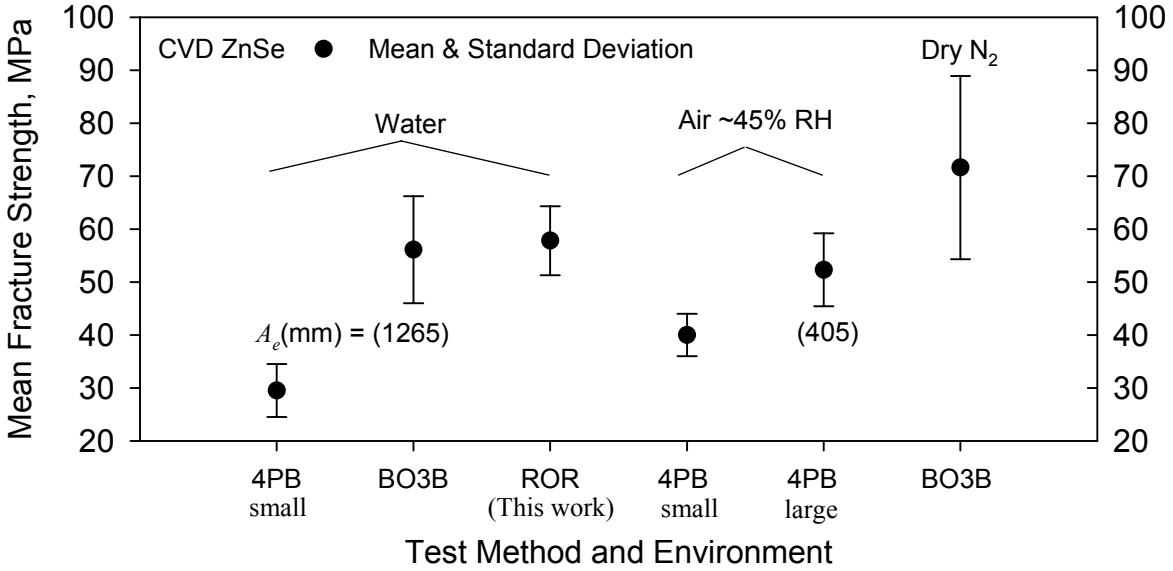

Figure 5.—Summary of published strength of CVD ZnSe (ref. 1). 4PB is four point bending; BO3B is point loading of a circular plate supported by 3 balls; ROR is concentric loading of a circular plate between two rings of different diameters; A_e is the Weibull effective area based on the Principal of Independent Action.

TABLE 2.—EQUIBIAXIAL STRENGTH OF ROHM AND HAAS CVD ZnSe.
TEST SPECIMENS WERE LOADED AT A RATE OF 316 N/s.

Specimen number	Specimen thickness, h mm	Specimen diameter, D mm	Young's modulus, E GPa	Poisson's ratio, v	Load diameter, D_L mm	Support diameter, D_S mm	Stress rate, $\dot{\sigma}$ MPa/s	Failure load, F N	Equibiaxial fracture strength, σ_f MPa	Estimated crack length, a	
										$a = c$ mm	$a = 0.1\ c$ mm
Tag 27335:											
11RH	4.037	63.39	74.2	0.31	25.446	50.808	9.93	1801	56.6	0.110	0.049
12RH	4.042	63.53	74.4	0.31	25.446	50.808	9.91	1653	51.8	0.025	0.011
13RH	4.022	63.53	74.6	0.31	25.446	50.808	10.00	1976	62.5	0.017	0.008
14RH	4.035	63.52	74.2	0.31	25.446	50.808	9.93	2003	63.0	0.018	0.008
15RH	4.005	63.53	74.4	0.31	25.446	50.808	10.08	1942	61.9	0.018	0.008
16RH	4.007	63.52	74.4	0.31	25.446	50.808	10.08	1992	63.5	0.017	0.007
Tag 27460:											
17RH	3.938	63.53	74.2	0.31	25.446	50.808	10.43	2155	71.1	0.013	0.006
18RH	3.936	63.53	74.2	0.31	25.446	50.808	10.44	1671	55.2	0.022	0.010
19RH	3.937	63.52	74.5	0.31	25.446	50.808	10.44	1629	53.8	0.022	0.010
20RH	3.967	63.53	74.2	0.31	25.446	50.808	10.27	1758	57.1	0.022	0.010
21RH	3.926	63.55	74.3	0.31	25.446	50.808	10.49	1960	65.1	0.018	0.008
22RH	3.949	63.52	74.6	0.31	25.446	50.808	10.39	1537	50.5	0.026	0.012
23RH	3.963	63.56	74.2	0.31	25.446	50.808	10.30	1472	48.0	0.028	0.013
24RH	3.973	63.51	74.4	0.31	25.446	50.808	10.26	1596	51.8	0.025	0.011
25RH	3.935	63.53	74.6	0.31	25.446	50.808	10.44	1655	54.7	0.022	0.010
							Average strength = 57.8 MPa				
							Standard deviation = 6.5 MPa				

Hardness

The hardness of polished and etch specimens was measured by using Vickers and Knoop indentation with a 15 s load duration. Due to the softness of ZnSe, measurements were made both at the loads required by ASTM C1326 and C1327 (refs. 7 and 8) and at lower loads. Because of the large grain size, the low load indentations were usually smaller than a single grain. Thus, to provide consistency and investigate the effect of grain orientation, grains with and without twins visible were indented. At least three tests were run per indentation load, but typically five to ten. The results are summarized in table 3. The 0.5 kg Knoop and Vickers hardness is 0.97±0.02 GPa.

In general, lower load indentation produced higher hardness values. Low load Vicker's indentation within grains produced the highest hardness values and the most scatter. The high average value for single grains appears to be at least partially an artifact of the low load rather than a reflection of single crystal hardness anisotropy, whereas the scatter is a reflection of anisotropy.

It should be noted that the hardness of CVD ZnSe is about one-twentieth of the sapphire being replaced (ref. 9), and about one-sixth of that of soda-lime-silicate glass. Thus the ZnSe window must be handled with great care.

TABLE 3.—HARDNESS OF CVD ZnSe AT 23 °C AND 50 PERCENT RELATIVE HUMIDITY

Load, *g*	Knoop hardness, *HK* GPa	Vickers hardness, *HV* GPa
25 (no twins)	----------	1.12±0.07[1]
50 (no twins)	1.10±0.10[2]	1.11±0.05[1]
25 (twins)[3]	----------	1.18±0.04[1]
50 (twins)	----------	1.15±0.04[1]
200	0.98±0.01	----------
500	0.97±0.02	0.97±0.02
1000	0.95±0.01[4]	0.96±0.02[5]

1. Indentations were within a single grain.
2. Indentations covered more than one grain. Both regions with twins and regions not displaying twins were indented.
3. Indentions diagonals were place at both 45 and 0/90° to the twins. No measurable difference was detected.
4. Slight cracking around indentation tips.
5. Cracking from indentation tips.

Grain Size

The measured strength and fracture toughness of ZnSe is a function of the grain size (refs. 10 and 11). To compare the current materials strength and grain size to that published, the grain size was measured in accordance with ASTM E8 (ref. 12) by using the linear intercept method. Sections oriented parallel and perpendicular to the growth direction were polished and etched for several minutes by using a mixture of 200 gms chromic acid, 15 gms Na_2SO_4, 50 ml HNO_3, and 900 ml H_2O. Figure 6 shows typical grain structure of the CVD ZnSe being used. The grain structure is complex, varies widely and heavy twinning is apparent. Regions of many grains with twins oriented toward the deposition direction were observed as well as regions containing more grains of an orientation that darkened upon etching, implying some heterogeneity. Although the average measured grain size is $\bar{l}$ = 43±9 μm, grains as large as 150 μm can be observed, again implying that single crystal properties should be used in design of structural components. A slight difference between measurements made parallel and perpendicular to the deposition plane was measured, ($\bar{l}_t$ = 42±2 versus $\bar{l}_p$ = 47±3 μm at 95 percent confidence). The results are compared to published values in figure 7.

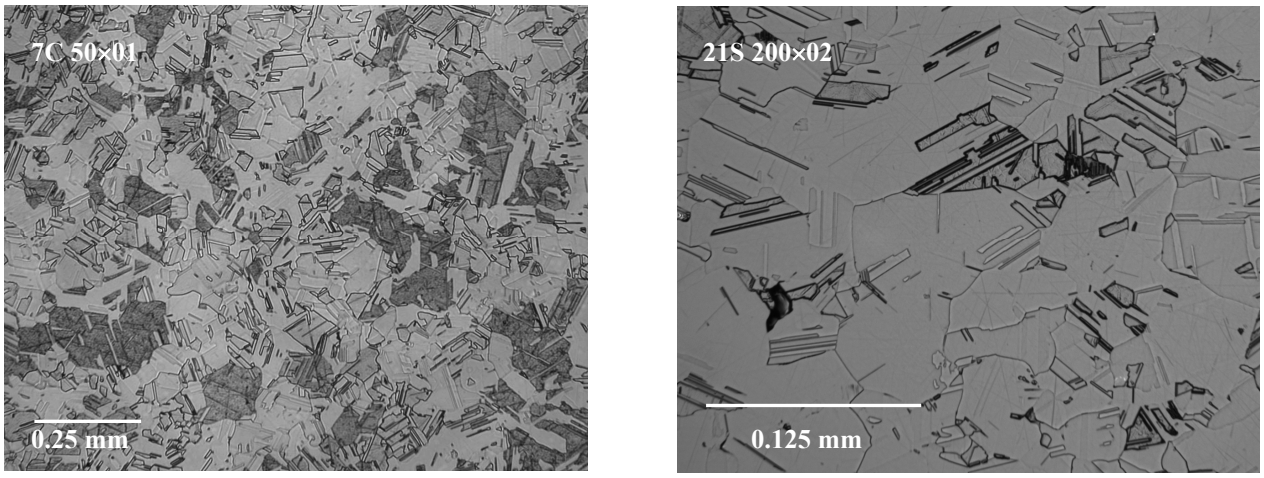

Figure 6.—Microstructure of CVD ZnSe.

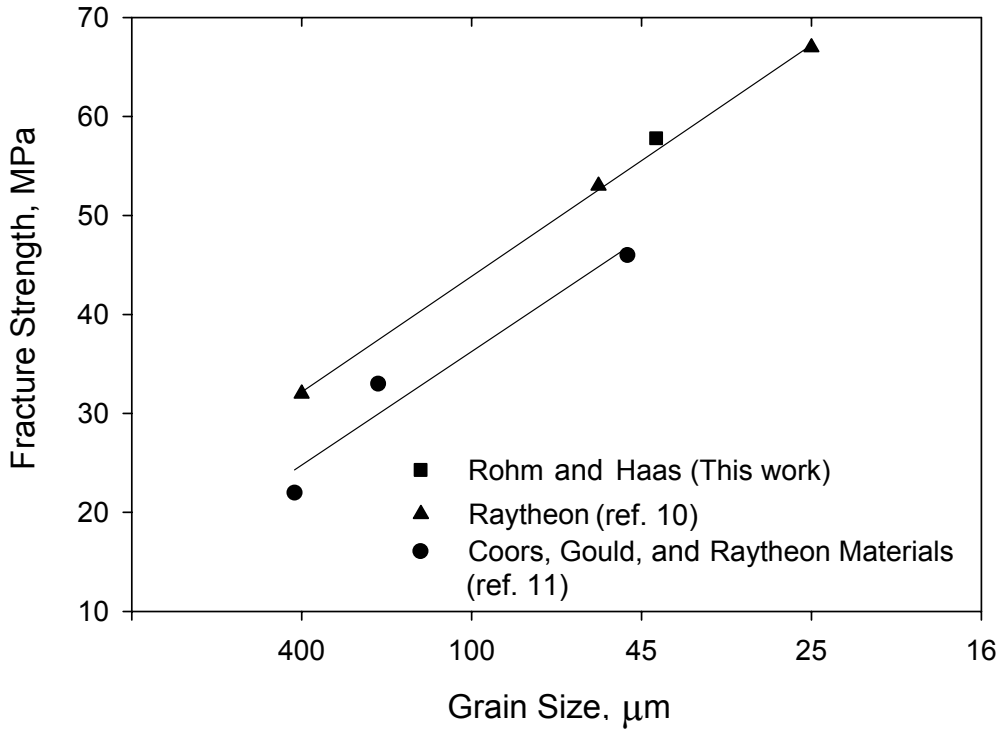

Figure 7.—Fracture strength as a function of grain size for CVD ZnSe made by various manufacturers.

Crack Branching Constants

Crack branching constants are useful in determining the nominal failure stress of components and estimating the presence of residual stresses in test specimens. The crack branching length is usually described by

$$\sigma_f = A_b r_b^{-0.5} \tag{2}$$

where σ_f is the fracture stress and A_b is the empirical constant corresponding to the branching boundary with radius r_b, as shown in figure 8. The exponent of –0.5 on r_b is a generally accepted value, but does vary somewhat. The branch lengths were measured on each specimen by optical microscopy, and the branching constant, A_b, was calculated by using four methodologies: (1) point wise estimation with equation (2); (2) nonlinear curve fit to equation (2) with and without assuming an exponent of $M = -0.5$; (3) by taking logarithms of equation (2) with and without assumption of $M = -0.5$ and applying linear regression:

$$\log \sigma_f = M \log r_b + \log A_b ; \tag{3}$$

and (4) by linear regression of the formula (ref. 13)

$$\sigma_f = A_b r_b^{-0.5} + \sigma_{th} \tag{4}$$

where σ_{th} has been interpreted as either a threshold stress for branching or a residual stress (refs. 13 and 14). Ideally, the branch length should be treated as the dependant variable rather than as the independent variable because it results from the applied load. However, the treatment is customarily done as shown in equations (2) to (4).

Three of the test specimens failed just outside of the load ring and one just inside the support ring. The specimen failing just inside the support ring did not exhibit branching before the crack intersected the test specimen edge. Estimations of A_b were made with and without the inclusion of these test specimens to determine the affect of a non-uniform stress state. For the specimen failing just inside the support ring, an elastic solution to calculate the edge stress was not available in the published literature, so the following solution was derived (ref. 15):

$$\sigma_r = \frac{3F(\nu - 1)\left(R_L^2 - R_S^2\right)\left(r^2 - R_D^2\right)}{4\pi h^2 R_D^2 r^2} \tag{5}$$

$$\sigma_\theta = \frac{3F(\nu - 1)\left(R_L^2 - R_S^2\right)\left(r^2 + R_D^2\right)}{4\pi h^2 R_D^2 r^2} \tag{6}$$

where σ_r and σ_θ are the radial and tangential stresses, respectively, between the test specimen edge and support ring, r is the radial failure position, R_S the support radius, R_L the load radius, R_D the specimen radius, h the thickness, and F the failure load. Equations (5) and (6) were found comparable to finite element analysis. The stress at the edge of the specimen is

$$\sigma_\theta = \frac{3F(\nu - 1)\left(R_L^2 - R_S^2\right)}{2\pi h^2 R_D^2}. \tag{7}$$

Figures 8 to 10 show the data plotted according to equations (2) to (4), and tables 4 and 5 summarize branch lengths and branch constants via the methods described. The figures indicate that the single specimen that failed at low local stresses (i.e., the stress at the point of failure) will influence the results particularly when curve fitting techniques are used.

Equations (2) to (4) result in a branching constant of $A_b \approx 1.0$ MPa$\sqrt{\text{m}}$ when M is taken as –0.5, with estimates from equation (4) invariably being the lowest. If M is determined via fitting, A_b increases to ~2 MPa$\sqrt{\text{m}}$, with an estimated $M \approx -0.4$. Consideration of the test specimen failing just inside the support ring tends to increase A_b, particularly when M is estimated from curve fitting. Equation (4) gives a $\sigma_{th} \approx 9$ MPa for all cases.

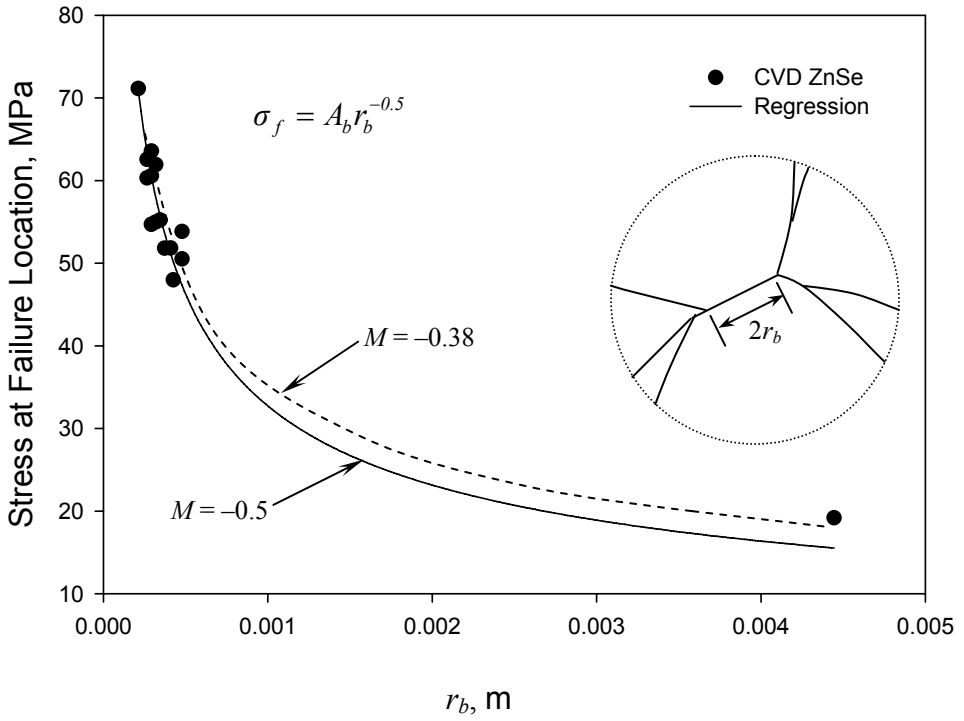

Figure 8.—Fracture strength as a function of crack branching length for CVD ZnSe.

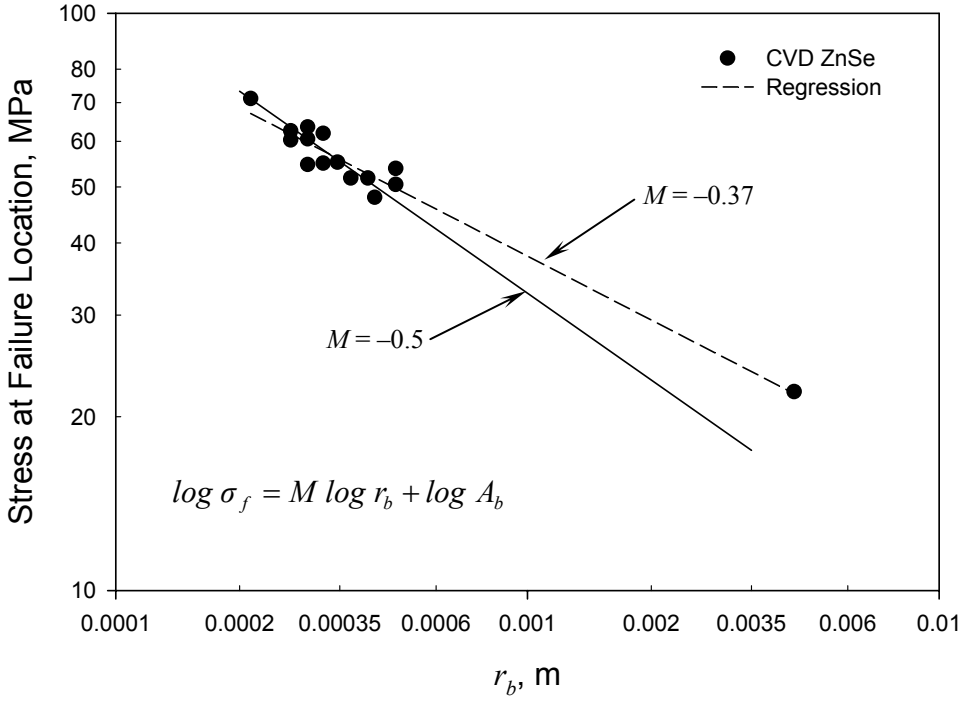

Figure 9.—Fracture strength as a function of crack branching length for CVD ZnSe.

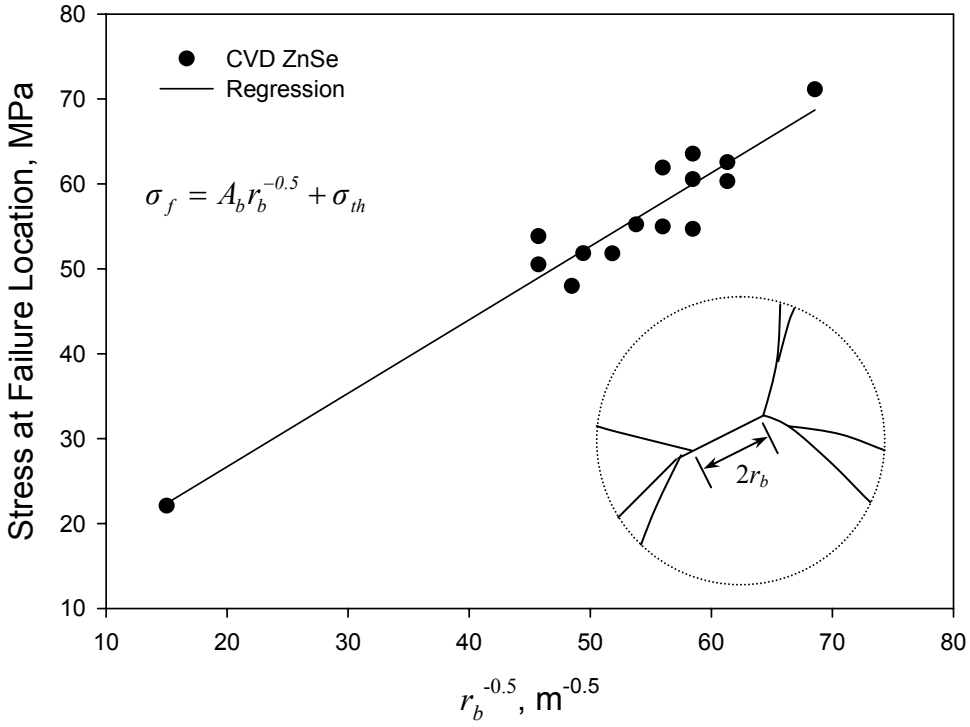

Figure 10.—Fracture strength as a function of crack branching length to the –0.5 power for CVD ZnSe.

The most sensitivity to the use of local stress as compared to equibiaxial stress for the specimens failing outside of the load ring was exhibited by equation (3) (e.g., when specimens 14, 20, and 21 are used with the equibiaxial stress, A_b = 1.9 MPa√m, whereas use of the local stress gives A_b = 2.4 MPa√m).

The most agreement between equations (2) to (4) occurs when the three specimens that failed just outside the load ring are used with the equibiaxial stress. This also produces the exponent closest to –0.5. This likely occurs because the actual stresses near the load ring are slightly higher than those calculated with the standard elastic solution (ref. 17) due to contact stresses, thereby decreasing the branch length. The specimen failing well outside the load ring was subjected to a near uniaxial stress state and yields an individual branching constant of A_b = 1.7 MPa√m, in good agreement with the reported value of 1.7 MPa√m for uniaxial stresses (ref. 16). It should be noted, however, that A_b values derived from uniaxial and biaxial tests have shown agreement, implying a single value of A_b regardless of stress state (ref. 18). Whether the significance of the agreement between this data point and the reported value for uniaxial testing is a coincidence or an indication of a difference between biaxial and uniaxial branching for ZnSe is unclear due to a lack of data. However, it should be noted that the branching occurred in an asymmetric fashion: the branch length toward the specimen center was 4.7 mm while branching away from the specimen center did not occur before the crack propagated 7.4 mm and traversed the specimen edge. If A_b is calculated using the static edge stress, the branch stress, or the stress at the origin with the respective branch lengths, A_b values of 1.5, 2.5, or 1.9 MPa√m result respectively (see table 4), implying a higher A_b for uniaxial states. However, the use of the static stresses calculated at the plate edge and the branch point are likely inappropriate because of the dynamics of fracture. Use of the stress at the point of failure and the branch length, which are the only well defined values, results in A_b = 1.7 MPa√m.

Besides considering the equibiaxial stress and local stress in calculation of A_b, estimates were made using a mode I equivalent stress based on the Principal of Independent Action (PIA). This usually increased the estimated value of A_b and decreased the estimated value of M, but did not result in better agreement

between the cases shown in table 5. Because only a single stress, rather than the stress components that makeup an equivalent stress, can be determined from a single equation such as (2), the use of an A_b value calculated with biaxial data and equation (2) may be the best approach when multiaxial stresses are considered likely.

For fractographic analysis of CVD ZnSe components subjected to a biaxial stress state, the branching constant is A_b = 1.0±0.1 MPa√m. Better estimates of the branch constant and distinction of the best technique would require much more data covering a larger range of failure stresses.

TABLE 4.—LOCAL STRESSES AND BRANCH LENGTHS FOR CVD ZnSe.

Specimen number	Equibiaxial fracture stress, σ_f MPa	Failure position, mm	Stress at failure location[a]		Branch length, r_b mm	Branch constant A_b MPa√m (via Eq. (2))
			Radial, σ_r MPa	Tangential, σ_θ MPa		
12RH	51.8	10.68			0.41	1.0
13RH	62.5	12.11			0.27	1.0
14RH	63.0	13.53	55.9	60.6	0.29	1.0
15RH	61.9	10.68			0.32	1.1
16RH	63.5	9.26			0.29	1.1
17RH	71.1	10.68			0.21	1.0
18RH	55.2	9.26			0.35	1.0
19RH	53.8	12.11			0.48	1.2
20RH	57.1	13.53	50.7	55.0	0.32	1.0
21RH	65.1	14.25	51.8	60.3	0.27	1.0
22RH	50.5	4.27			0.48	1.1
23RH	48.0	11.40			0.43	1.0
24RH	51.8	10.68			0.37	1.0
25RH	54.7	9.97			0.29	0.9
Calculations for no. 11RH						
Edge Stress	56.6	24.36	0	17.5	7.3	1.5
Local Stress	" "	" "	–1.7	24.8	4.7	1.7
Local Stress	" "	" "	" "	" "	6.0[b]	1.9
Branch Stress[c]	" "	" "	15.8	36.9	4.7	2.5

[a]Values are not shown for specimens that failed in the central region.
[b]Average of lengths from origin to branch point and from origin to specimen edge.
[c]The stresses calculated at the point of branching and at the specimen edge were based on static elastic analysis and thus are likely inappropriate because of the dynamics of failure.

TABLE 5.—BRANCH CONSTANTS FOR CVD ZnSe AS CALCULATED WITH EQUATIONS (1) TO (3).

Equation[a]	M	A_b MPa√m	σ_{th} MPa	r^2
Without no. 11RH, 14RH, 20RH, and 21RH				
(2) point wise	–0.5	1.0±0.1	-----	----
(2) nonlinear	–0.5	1.0±0.6	-----	0.76
(2) nonlinear	–0.43±0.07	1.9±1.1	-----	0.78
(3)	–0.5	1.0±0.1	-----	0.72
(3)	–0.41±0.08	2.2±1.3	-----	0.76
(4)	–0.5	0.9±0.2	9.1	0.79
With no. 14RH, 20RH, 21RH, and equibiaxial stress				
(2) point wise	–0.5	1.0±0.1	-----	----
(2) nonlinear	–0.5	1.0±0.6	-----	0.88
(2) nonlinear	–0.44±0.06	1.7±1.9	-----	0.89
(3)	–0.5	1.0±0.1	-----	0.75
(3)	–0.43±0.07	1.9±1.0	-----	0.78
(4)	–0.5	0.9±0.1	7.3	0.80
With no. 14RH, 20RH, 21RH, and local stress				
(2) point wise	–0.5	1.0±0.1	-----	----
(2) nonlinear	–0.5	1.0±0.6	-----	0.85
(2) nonlinear	–0.41±0.07	2.1±1.1	-----	0.87
(3)	–0.5	1.0±0.1	-----	0.69
(3)	–0.39±0.06	2.4±1.2	-----	0.75
(4)	–0.5	0.8±0.1	10.4	0.77
With no. 11RH, 14RH, 20RH, 21RH, and local stress				
(2) point wise	–0.5	1.1±0.1	-----	----
(2) nonlinear	–0.5	1.0±0.5	-----	0.89
(2) nonlinear	–0.39±0.04	2.6±0.9	-----	0.92
(3)	–0.5	1.0±0.1	-----	0.83
(3)	–0.37±0.02	3.0±0.5	-----	0.96
(4)	–0.5	0.9±0.1	9.4	0.93

[a]Equation (2) is $\sigma_f = A_b r_b^{-0.5}$; Equation (3) is $\log \sigma_f = M \log r_b + \log A_b$; Equation (4) is $\sigma_f = A_b r_b^{-0.5} + \sigma_{th}$;
r^2 = Pearson coefficient squared.

Summary and Conclusions

The properties of CVD ZnSe were measured in order to determine design allowables for the FEANICS module. The measured values were in good agreement with values reported in the 1970's. The average Young's modulus, Poisson's ratio, equibiaxial fracture strength, flaw size, grain size, Knoop hardness, Vicker's hardness, and branching constant for the CVD ZnSe were E = 74.3±0.1 GPa, ν = 0.31, $\overline{\sigma}_f$ = 57.8±6.5 MPa, a = 21 ± 4 μm, $\bar{l}$ = 43±9 μm, HK0.5/15 = 0.97±0.02 GPa, HV0.5/15 = 0.97±0.02 GPa, and A_b = 1.0±0.1 MPa√m. The hardness of CVD ZnSe is about one-twentieth of sapphire, and thus the ZnSe window must be handled with care. Due to the occasional presence of very large grains and the small inherent flaw size, it is recommended that the single crystal properties be used in design of structural components made from CVD ZnSe. In order to calculate the stresses between the support ring and the edge of circular plates loaded between concentric rings, a stress solution was derived.

Recommendations

Test witness coupons that are manufactured along with the flight window(s). Development of a fine grained transparent ZnSe would enhance window fracture toughness, fracture strength, and slow crack growth resistance.

References

1. J.A. Salem, "Estimation of ZnSe Crack Growth Properties for Design of the FEANICS Windows," NASA/TM—2005-213359 (2005).
2. ASTM C1499–01 "Determination of Monotonic Equibiaxial Flexural Strength Advanced Ceramics," in *Annual Book of ASTM Standards*, vol. 15.01, American Society for Testing and Materials, West Conshohocken, Pennsylvania (2004).
3. ASTM C1259–94, "Standard Test Method for Dynamic Young's Modulus, Shear Modulus, and Poisson's Ratio for Advanced Ceramics by Impulse Excitation of Vibration," in *Annual Book of ASTM Standards*, vol. 15.01, American Society for Testing and Materials, West Conshohocken, Pennsylvania, (2004).
4. J.A. Salem and A. Singh, "Polynomial Expressions for Estimating Elastic Constants From the Resonance of Circular Plates," NASA/TM—2005-213843, (2005).
5. A.G. Evans and H. Johnson, "A Fracture-Mechanics Study of ZnSe for Laser Window Applications," *J. Am. Ceram. Soc.,* vol. 58, no. 5–6, pp. 244–249 (1975).
6. G.A. Graves, D.E. McCullum, and J.M. Wimmer: Exploratory Development and Investigation of the Thermal, Electrical, Mechanical, and Physical Properties of Infrared Laser Window and I–R Transmitting Materials; Final Technical Report. AFML–TR–77–23, UDRI–TR–77–06, 1977. Available from the NASA Center for Aerospace Information.
7. ASTM C1326, "Standard Test Methods for Knoop Indentation Hardness of Advanced Ceramics," in *Annual Book of ASTM Standards*, vol. 15.01, American Society for Testing and Materials, West Conshohocken, Pennsylvania (2005).
8. ASTM C1327, "Standard Test Methods for Vickers Indentation Hardness of Advanced Ceramics," in *Annual Book of ASTM Standards*, vol. 15.01, American Society for Testing and Materials, West Conshohocken, Pennsylvania (2005).
9. J.A. Salem, "Slow Crack Growth and Fracture Toughness of Sapphire for the International Space Station Fluids and Combustion Facility," NASA/TM—2006-214023 (2006).
10. P. Miles "High Transparency Infrared Materials—A Technology Update," *Opt. Eng.*, vol. 15, no. 5, pp. 451–459 (1976).
11. J.C. Wurst and T.P. Graham: Thermal, Electrical, and Physical Measurements of Laser Window Materials; Final Report. AFML–TR–75–28, UDRI–TR–75–06, 1975. Available from the NASA Center for Aerospace Information.
12. ASTM E112, "Standard Test Methods for Determining Average Grain Size," in *Annual Book of ASTM Standards*, vol. 03.01, American Society for Testing and Materials, West Conshohocken, Pennsylvania (2005).
13. J.B. Quinn, "Extrapolation of Fracture Mirror and Crack-Branch Sizes to Large Dimensions in Biaxial Strength Tests of Glass," *J. Am. Ceram. Soc*., 82 [8], pp. 2126–32 (1999).
14. J.J. Mecholsky, Jr., S.W. Freiman, and R.R. Rice, "Fractographic Analysis of Ceramics," pp. 336–379 in *Fractography in Failure Analysis, Special Technical Publication 645*, B.M. Strauss and W.H. Cullen, eds., American Society for Testing and Materials, West Conshohocken, PA, (1977).
15. J.M. Manderscheid, private communication, NASA Glenn Research Center, June 20, 2005.
16. J.J. Mecholsky, Jr., S.W. Freiman, and R.W. Rice, "Fractographic Analysis of Ceramics," *J. Materials Science,* 11, pp. 1310–1319 (1976).
17. J.A. Salem and L.M. Powers, "Guidelines for the Testing of Plates" pp. 357–364 in Proceedings of the 27th International Cocoa Beach Conference on Advanced Ceramics and Composites: B, *Ceramic Engineering and Science Proceedings*, vol. 24, no. 4, Waltraud M. Kriven and H.T. Lin, editors (January, 2003).
18. J.J. Mecholsky, Jr., and R.W Rice, "Fractographic Analysis of Biaxial Failure in Ceramics," pp. 185–193 in *Fractography of Ceramic and Metal Failures, Special Technical Publication 827*, American Society for Testing and Materials, West Conshohocken, Pennsylvania (1984).

Appendix—Equibiaxial Fracture Strength Testing Report

1. Test Date: July 9th and 12th, 2004.
2. Rohm Haas CVD ZnSe produced in April of 2004. Material may have been produced in two lots (Tag no. 27355 and no. 27460 delivered on 4/07/05 and 4/16/05, respectively).
3. Polished according to the specifications in figure 2. Rohm and Haas declined to disclose all stages of polishing as it is proprietary. Diamond grinding followed by polishing with an alumina slurry was indicated. A 10 min soak in water was performed prior to testing.
4. Instron 8521 servo-hydraulic test frame with Instron 10KN load cell no. 1462.
5. Test fixtures were marging steel hardened to 50 RC. The load ring diameter was 25.44 mm and the support ring diameter was 50.81 mm. The cross section radius of the ring contact points were 4 mm.
6. Two 0.005 in. grafoil layers were used between the load fixtures and the test specimen. Also, the compression sides of the test specimens were covered with cellophane tape.
7. Test environment was distilled, deionized water from the distillation unit in building 49. Ambient temperature was 76 °F with 45 percent RH.
8. Test mode was load control with a load rate of 316 N/s resulting in a nominal stress rate of 10 MPa/s.
9. The measured Poisson's ratio and Young's modulus are summarized in table 1.
10. The average diameter and thickness of each test specimen is summarized in table 2.
11. The preload applied to each test specimen was 10 N. The resultant pre-stress was 0.3 MPa. See table 2.
12. The breaking load and equibiaxial flexural strength of each test specimen is summarized in table 2.

REPORT DOCUMENTATION PAGE

Form Approved
OMB No. 0704-0188

1. AGENCY USE ONLY (*Leave blank*)	2. REPORT DATE	3. REPORT TYPE AND DATES COVERED
	February 2006	Technical Memorandum

4. TITLE AND SUBTITLE

Mechanical Characterization of ZnSe Windows for Use With the Flow Enclosure Accommodating Novel Investigations in Combustion of Solids (FEANICS) Module

5. FUNDING NUMBERS

WBS–22–400–35–40–07

6. AUTHOR(S)

Jonathan A. Salem

7. PERFORMING ORGANIZATION NAME(S) AND ADDRESS(ES)

National Aeronautics and Space Administration
John H. Glenn Research Center at Lewis Field
Cleveland, Ohio 44135–3191

8. PERFORMING ORGANIZATION REPORT NUMBER

E–15435

9. SPONSORING/MONITORING AGENCY NAME(S) AND ADDRESS(ES)

National Aeronautics and Space Administration
Washington, DC 20546–0001

10. SPONSORING/MONITORING AGENCY REPORT NUMBER

NASA TM—2006-214100

11. SUPPLEMENTARY NOTES

Responsible person, Jonathan A. Salem, organization code RXL, 216–433–3313.

12a. DISTRIBUTION/AVAILABILITY STATEMENT

Unclassified - Unlimited
Subject Category: 27

Available electronically at http://gltrs.grc.nasa.gov

This publication is available from the NASA Center for AeroSpace Information, 301–621–0390.

12b. DISTRIBUTION CODE

13. ABSTRACT ***(Maximum 200 words)***

Mechanical and physical properties of ZnSe windows to be used with the FEANICS (Flow Enclosure Accommodating Novel Investigations in Combustion of Solids) experiments were measured in order to determine design allowables. The average Young's modulus, Poisson's ratio, equibiaxial fracture strength, flaw size, grain size, Knoop hardness, Vicker's hardness, and branching constant were 74.3 ± 0.1 GPa, 0.31, 57.8 ± 6.5 MPa, 21 ± 4 mm, 43 ± 9 μm, 0.97 ± 0.02 GPa, 0.97 ± 0.02 GPa, and 1.0 ± 0.1 MPa$\sqrt{m}$, respectively. The properties of current ZnSe made by chemical vapor deposition are in good agreement with those measured in the 1970's. The hardness of CVD ZnSe windows is about one-twentieth of the sapphire window being replaced, and about one-sixth of that of window glass. Thus the ZnSe window must be handled with great care. The large grain size relative to the inherent crack size implies the need to use single crystal crack growth properties in the design process. In order to determine the local failure stresses in one of the test specimens, a solution for the stresses between the support ring and the edge of a circular plate load between concentric rings was derived.

14. SUBJECT TERMS

Zinc selenide; flexural strength; Modulus of elasticity; Poisson ratio; Hardness; Stress corrosion; Weibull; Structural reliability; Microstructure; Grain size; Branching constant; Laser window; Pressure chambers

15. NUMBER OF PAGES

22

16. PRICE CODE

17. SECURITY CLASSIFICATION OF REPORT	18. SECURITY CLASSIFICATION OF THIS PAGE	19. SECURITY CLASSIFICATION OF ABSTRACT	20. LIMITATION OF ABSTRACT
Unclassified	Unclassified	Unclassified	